Improved surface wave tomography: Imposing wavelength-based weights

IMPROVED SURFACE WAVE TOMOGRAPHY: IMPOSING WAVELENGTH-BASED WEIGHTS.

F. Khosro Anjom, L.V. Socco
DIATI, Politecnico di Torino, Turin, Italy

Introduction. Surface wave tomography (SWT) is a well-stablished method in local and global scale, to reconstruct the shear wave velocity (VS) model of the near-surface (Papadopoulou *et al*., 2019; Socco *et al*., 2014; Picozzi *et al*., 2009) and crust/upper mantle (Wespestad *et al*., 2019; Bao *et al*., 2015; Boiero, 2009; Yao *et al*., 2006). Conventionally, SWT methods are integrated with a two-station processing method, by which the surface-wave average dispersion curves (DCs) are acquired along different paths. In the two-station data processing scheme, commonly, the DCs are estimated uniformly in frequency. However, uniform sampling of the phase velocities in frequency, prompts a non-uniform sampling in wavelength. Consequently, the DCs will contain lower population of data points for the large wavelengths compared to shorter wavelength portion. Since the investigation depth of the surface waves is directly related to the wavelength (Yao *et al*., 2006; Socco *et al*., 2010), having larger distribution of data points for short wavelengths will drive the inversion to the shallowest portion of the model. In other words, high frequency/short-wavelength data points will rule the inversion and they will limit the investigation depth. To overcome this problem and improve the investigation depth, we propose imposing weights to the data points of the DCs, according to the wavelength distribution.

Here, we explain the method to impose wavelength-based weights to the data points for the inversion. Then, we show an application of surface wave tomographic inversion to a synthetic data set, where the wavelength-based weights are assigned to the dispersion data points, and we compare it to the result of the inversion without imposing any weight.

Method. Considering the average DCs of multiple paths, first, we transform the average DCs to wavelength-phase velocity domain by dividing phase velocity and frequency elements. Then, for each point of the average DC, we compute the corresponding weight as the distance to the closest data point in terms of wavelength. We define the misfit function Q in scheme of weighted least square of the average slowness ($\frac{1}{Phase\ Velocity}$), as:

$$Q = [\ (\mathrm{S}_{true} - \mathrm{S}_M)^T W\ (\mathrm{S}_{true} - \mathrm{S}_M)]^{0.5}, \quad (1)$$

where S_{true} and S_M are the true and synthetic average slowness of the paths, respectively, and W is the diagonal matrix of wavelength-based weights corresponding to the data points. We use a damped least square Levenberg-Marquandt method (Boiero, 2009) to minimize the misfit function Q iteratively and update the model parameters at each iteration as:

$$M_{n+1} = M_n + [(G^T W G + \lambda I)^{-1} \times (G^T W \left(\mathrm{S}_{obs} - \mathrm{S}_{(Mn)}\right))], \quad (2)$$

where M_n and M_{n+1} are the current and the new model parameters, respectively. λ is the damping factor which attempts to trade off the accuracy and feasibility of the solution, and G is the Jacobian representing the sensitivity matrix.

Synthetic Example. The initial model of the synthetic example is consisting of 60 1D layered models evenly spaced along a 2 km line. Each model includes 8 layers over the half-space, where the density and Poisson's ratio of all layers are constant and equal to 2800 kg/m^3 and 0.3, respectively. The initial model was strongly perturbed (20%) by altering the 1D VS models negatively and positively to form a checkerboard 2D model (true model). In Figs 1a and 1b, we show the initial VS model and the scheme of the perturbation, respectively. In Fig. 1c, we show the perturbed (true) VS model after applying the perturbation (Fig. 1b) to the initial model (Fig. 1b).

To achieve a large and uniform data coverage, we defined 240 paths, uniformly distributed

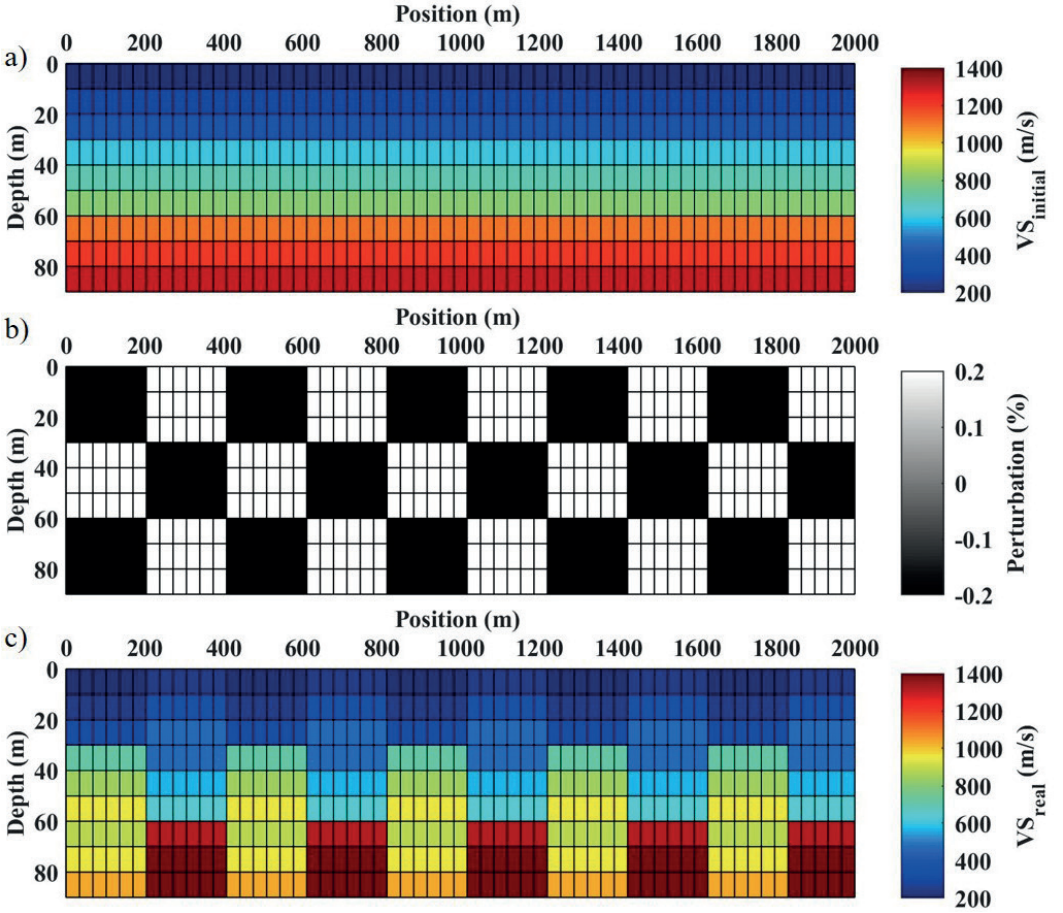

Fig. 1 - (a) The initial VS model. (b) The perturbation map in percentage where the black color shows a 20% negative perturbation and the white color represents a 20% positive perturbation. (c) The perturbed (true) model.

along the entire model. To obtain the true average DCs corresponding to each path, we discretized each path (every 5 m) and we computed the average slowness from 3 to 50 Hz using the DCs of the closest 1D models to each point of the discretized path. In Figs 2a and 2b, we show the true average DCs in the phase velocity-frequency and phase velocity-wavelength

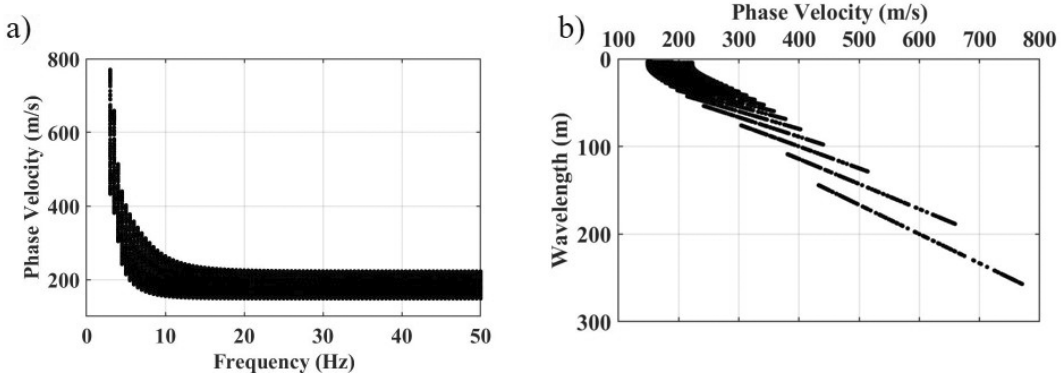

Fig. 2 - The dispersion curves corresponding to the ray paths defined for the true model (Fig. 1b): (a) The phase velocities against frequency. (b) The phase velocities against wavelength.

domain, respectively. The non-uniform sampling of the wavelengths is evident in Fig. 2b, where the large-wavelength data points are more distant from each other compared to the short-wavelength data points.

Starting from the initial model (Fig. 1a) and the true average DCs corresponding to the paths (Fig. 2a), we performed an inversion without considering any weight for the data points. In Figs 3a and 3b, we compare the real VS model with the estimated VS model from non-weighted inversion. We performed a second inversion, where we assigned weights to data-points of the true DCs. The weights were obtained as the distance between the wavelengths of the data points (Fig. 2b). In Fig. 3c, we show the estimated VS model of the weighted inversion. Comparing the two inversions (Figs 3b and 3c), the non-weighted inversion shows a low resolution in recovering the true VS model between depths 30 to 40 m, and almost no resolution below 40 m, while the estimated VS model from the wavelength-based weighted inversion shows very good resolution up to 60 m. Below 60 m, the weighted inversion shows almost no changes compared to the initial model.

Conclusion. The SWT is inherently a very powerful tool to estimate VS with high resolution, if an adequate coverage of the data is available. The investigation depth of the inversion can be enhanced, by assigning wavelength-based weights to the data points prior to the inversion.

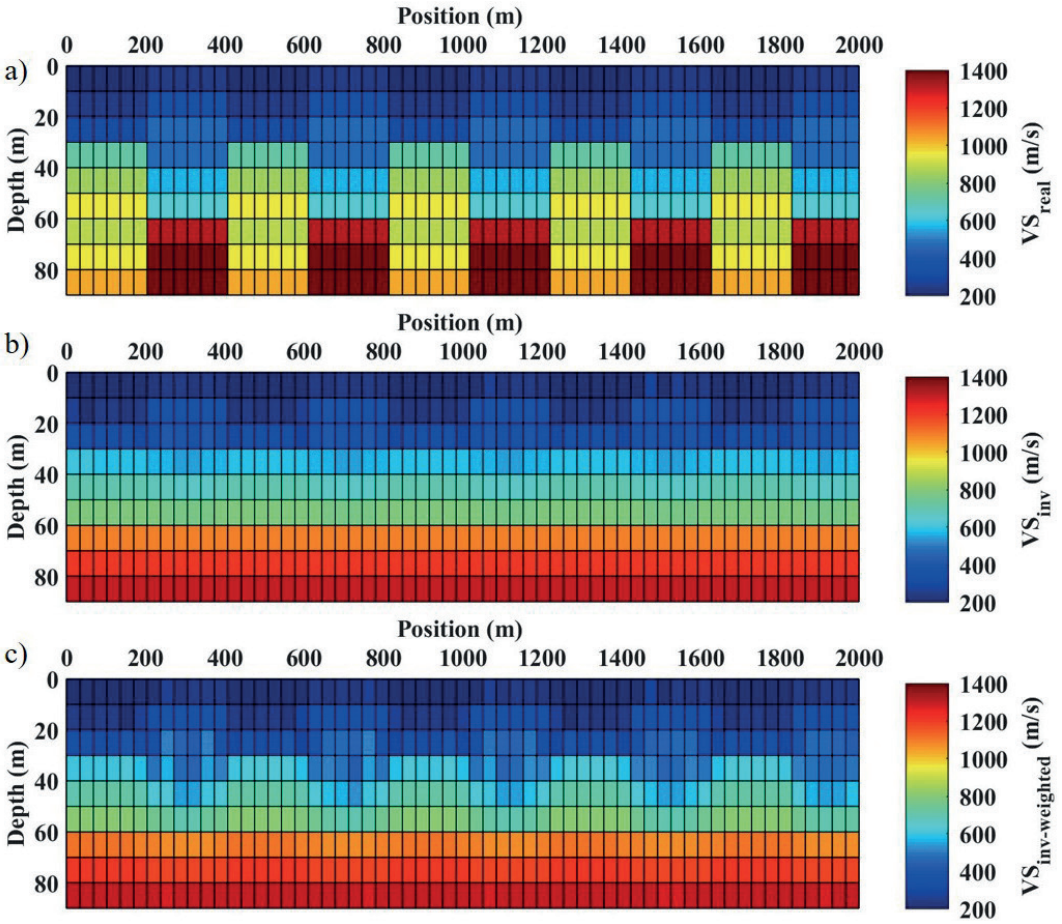

Fig. 3 - The real VS model compared with the estimated VS models using non-weighted and weighted inversions (a) The real model. (b) The estimated VS model using non-weighted inversion. (c) The estimated VS model using weighted inversion.

Specifically, the synthetic test shows more than 50% increase of the investigation depth, when wavelength-based weights are imposed. In the future, we will perform the wavelength-based weighted SWT on the real data.

Acknowledgments. The first author would like to thank TOTAL E&P for supporting his PhD.

References

Bao, X., Song, X. and Li, J.; 2015: High-resolution lithospheric structure beneath Mainland China from ambient noise and earthquake surface-wave tomography., Earth and Planetary Science Letters, 417, 132-141, doi: 10.1016/j.epsl.2015.02.024

Boiero, D.; 2009: Surface wave analysis for building shear wave velocity models., PhD thesis, Politecnico di Torino.

Papadopoulou, M., Da Col, F., Socco, L.V., Hu, S., Bäckström, E., Schön, M., Marsden, P. and Malehmir, A.; 2019: Surface-Wave Tomography at Mining Sites - A Case Study from Central Sweden., 25th European Meeting of Environmental and Engineering Geophysics, doi: 10.3997/2214-4609.201902464

Picozzi, M., Parolai, S., Bindi, D. and Strollo, A.; 2009: Characterization of shallow geology by high-frequency seismic noise tomography., Geophysical Journal International, 176(1), 164-174, doi: 10.1111/j.1365-246X.2008.03966.x

Socco, L.V., Boiero, D., Bergamo, P. and Garofalo, F.; 2014: Surface wave tomography to retrieve near surface velocity models., SEG, doi: 10.1190/segam2014-1278.1

Socco, L.V., Foti, S. and Boiero, D.; 2010: Surface-wave analysis for building near-surface velocity models—established approaches and new perspectives, Geophysics, 75(5), A83–A102. doi: 10.1190/1.3479491

Wespestad, C.E., Thurber, C.H., Andersen, N.L, Singer, B.S., Cardona, C., Zeng, Z., Bennington, N.L., Keranen, K., Peterson, D.E., Cordell, D. Unsworth, M., Miller, C. and Jones, G.W.; 2019: Magma Reservoir Below Laguna del Maule Volcanic Field, Chile, Imaged With Surface-Wave Tomography. JGR Solid Earth, 124(3), 2858-2872, doi: 10.1029/2018JB016485.

Yao, H., van der Hilst, R.D. and de Hoop, M.V.; 2006: Surface-wave array tomography in SE Tibet from ambient seismic noise and two-station analysis – I. Phase velocity maps, Geophysical Journal International,166(2), 732-744, doi: 10.1111/j.1365-246X.2006.03028.x

A NEW MULTI-METHOD APPROACH TO MONITOR THE STRESS STATE IN A ROCK MASS: THE CASE OF SAN BENEDETTO TUNNEL, CENTRAL ITALY

P. Luiso[1], C. De Paola[1,2], D. Di Massa[1], D. Fiore[1], S. Candela

[1] SOCOTEC Italia Srl - registered office, Lainate, Italy

[2] Dipartimento di Scienze della Terra, dell'Ambiente e delle Risorse, Università degli Studi «Federico II», Naples, Italy

Introduction. The combined analysis between resistivity/seismic tomographies and GPR surveys have long been used to investigate the first meters of subsoil, mainly to search and analyse lithological changes, landslides (Philips *et al*., 2019 and references therein) fractures (e.g. Sibula *et al*., 2017), the presence of water infiltration (e.g. Yusofl *et al*., 2017). In the last ten years some geophysicist used the electrical resistivity and refraction seismic tomographies (with GPR survey support) to monitoring the behaviour of the rock mass fixing electrodes in a series of close holes drilled vertically in the rock wall (Bàrta *et al*., 2010; Liu *et al*., 2013; Rathod *et al*., 2019; Singer *et al*., 2010; Tosti *et al*., 2019).

We here present a new methodology tested in the San Benedetto tunnel, crossed by the fault plane, that connects Norcia to Arquata del Tronto cities, on the border between Abruzzo and Molise regions, central Italy. The tunnel, damaged by the 30 October 2016 earthquake with M_w 6.5 (Villani *et al*., 2018) localized 4 km from Norcia (central Italy), was affected by coesismic fractures, a 10-20 cm displacement (Galli *et al*., 2019) and serious damage to the concrete